International Journal of Recent Technology and Engineering (IJRTE)
ISSN: 2277-3878, Volume-8 Issue-3, September 2019

Geometrical Design of a Rotor Blade for a Small Scale Horizontal Axis Wind Turbine

R Supreeth, A Arokkiaswamy, Nagarjun J Raikar, Prajwal H P, Sudhanva M

Abstract*: *In the present study, Blade Element Momentum theory (BEMT) has been implemented to heuristically design a rotor blade for a 2kW Fixed Pitch Fixed Speed (FPFS) Small Scale Horizontal Axis Wind Turbine (SSHAWT). Critical geometrical properties viz. Sectional Chord c_i and Twist distribution θ_{Ti} for the idealized, optimized and linearized blades are analytically determined for various operating conditions. Results obtained from BEM theory demonstrate that the average sectional chord c_i and twist distribution θ_{Ti} of the idealized blade are 20.42% and 14.08% more in comparison with optimized blade. Additionally, the employment of linearization technique further reduced the sectional chord c_i and twist distribution θ_{Ti} of the idealized blade by 17.9% and 14% respectively, thus achieving a viable blade bounded by the limits of economic and manufacturing constraints. Finally, the study also reveals that the iteratively reducing blade geometry has an influential effect on the solidity of the blade that in turn affects the performance of the wind turbine.

Keywords: Blade Element Momentum Theory, Chord Distribution, Renewable Energy, Solidity, Twist Distribution, Wind Energy

I. INTRODUCTION

Discovery of fossil fuels and their utilization as energy sources has been the greatest contribution of mankind to the society. Since time immemorial, energy has been an important entity instrumental in transcending a raw agrarian culture to a technologically advanced civilization. From the time of realization, till date, fossil fuels have been the world's primary source of energy for power generation responsible in fuelling the socio-economic development of the world [1].

Manuscript published on 30 September 2019
* Correspondence Author
R Supreeth*, Research Scholar, Department of Aeronautical Engineering, Dayananda Sagar College of Engineering, Assistant Professor, Department of Aerospace Engineering, Rashtreeya Vidyalaya College of Engineering, Bengaluru, India. Email: supreethr@rvce.edu.in
A Arokkiaswamy, Department of Aeronautical Engineering, Dayananda Sagar College of Engineering, Bengaluru, India.
Email: swamy.aroks@gmail.com
Nagarjun J Raikar, Department of Aerospace Engineering, Rashtreeya Vidyalaya College of Engineering, Bengaluru, India.
Email: nagarjunjr.ae15@rvce.edu.in
Prajwal H P, Department of Aerospace Engineering, Rashtreeya Vidyalaya College of Engineering, Bengaluru, India.
Email: prajwalhp.ae15@rvce.edu.in
Sudhanva M, Department of Aerospace Engineering, Rashtreeya Vidyalaya College of Engineering, Bengaluru, India. Email: sudhanvam97@gmail.com

Majority of the global energy demands are being satiated by conventional fossil fuel sources like coal, petroleum, natural gas etc. According to the energy information administration, around 80% of the world's energy demands are being met by fossil fuels alone [2]. Based on the estimates, the global consumption of fossil fuel resources in 2016 was 1, 32,051TWh that surged by 2.1 percent in 2017 [3]. Such prodigious use of fossil fuels has tremendously inflated the global carbon emissions that have created an irreparable harm on the entire ecosystem [4]. Nine billion tons of carbon emissions recorded in 1950 has shot up to a colossal 34 billion metric tons in 2015 and is likely to reach 45 billion by 2040[5-7]. Unabated dependency on fossil fuel has estimated to escalate the earth's average temperature by 7^0C by the turn of this century [8]. To prevent the appalling consequence, there is an imminent requirement to exploit all renewable energies [9]. Comparatively, the time tested developments in the field of wind energy has designated the wind turbines to be ideal candidates as a prudent replacement for traditional fossil fuels [10].

Through centuries, humans have been harnessing energy from the wind and the concept is not new to mankind. Wind energy was presumed to be first used for propelling ships through the deployment of wind sails. Later, the idea was extended for the establishment of wind mills whereby the kinetic energy of the moving wind was converted into useful mechanical energy for grinding grains, pumping water and so on [11]. Over years, the influence of Industrial revolution as well as the changing world dynamics dictated by oil rich nations, wind mills were subsequently transformed into machines producing electricity. Since the birth of industrial revolution, wind turbines have evolved as perfect candidates for generating useful electrical energy beyond just pumping water and grinding grains [11]. Advancement in the field of materials, computational capabilities, data acquisition, vibrations control etc., has collectively elevated the upward limit of the wind turbine in terms of power production. In 2010, the global cumulative installed wind power capacity was around 200GW. By the end of 2017 the installed capacity stood at a massive 539GW [12].

Effectively capturing energy from the moving wind entirely depends on the geometrical design of the rotor blade [13]. Majorly, blade forms the active component of any wind turbine system and furnishing an appropriate design is of paramount importance to maximize the power output. Arriving at efficient blade geometry is not a straightforward process that can be seldom achieved in a single step. As a general practice, realizing a final geometry is an iterative process involving several substeps.

The design of a rotor blade is governed by the principles of aerodynamics that can be comprehended by the application of Blade Element Momentum theory (BEMT) [14]. The current research work employs the BEM theory for developing effective blade geometry through a sequential process without appraising the blade performance.

The blade under consideration is for a fixed pitch fixed speed (FPFS) small scale horizontal axis stall controlled wind turbine with rated power of 2kW. Efforts have been made to understand the distinctive steps involved in BEMT yielding geometrically diverse derivatives of the blade due to the impending effects of wake ω, drag C_d, tip losses F_i and linearization. The geometrical deviations of the blade from the idealized conditions are analyzed through sectional chord c_i and twist distribution θ_{Ti} pattern. Consecutive steps of BEMT embraced in this research work aims to provide step by step guidelines for accomplishing final blade geometry with good aerodynamic and structural properties. Lastly, comparative studies will be undertaken to highlight the percentage of deviations in terms of chord c_i and twist distributions θ_{Ti} across all blade profiles.

Prasad et al. [15] observed the aerodynamic characteristics of NACA 4412 and NACA4415 airfoils by remodifying its thickness. Results showed that the airfoil with 30% varying thickness demonstrated better aerodynamic characteristics compared to the baseline airfoil. Burdett et al. [16] extensively validated the aerodynamic results of S823 and E387 airfoils invoked from PROFIL and XFOIL numerical codes with the experimental data. The research work shows that the design angle of attack estimated by numerical simulations were around 2.5% lesser than the experimental techniques. Chaudhary et al. [17] conducted aerodynamic analysis on NACA 63415 and NACA 63412 airfoils over a range of angles of attack at Re=1x106 using ANSYS/FLUENT software. Contrastingly, NACA 63415 displayed a better L/D ratio compared to NACA 63412 and recommended to be suitable for the design of rotor blades. As reported by Kumar et al. [18] SG6040, SG6041, SG6050, SG6043, E216, E555, E407, NREL and NACA 63-415 would best fit for a small scale HAWT rotor blade design. As per the study, it was postulated that a thick airfoil is of paramount importance for root section and thin airfoil is always preferred for the primary regions of the rotor blade. Giguere et al. [19] designed four airfoils, specifically for low Re applications namely, SG6041, SG6042, SG6043 and SG6040. The designed airfoils were found to perform well in the given range of Reynolds number and suggested to be ideal for wind turbines applications. Wisniewski et al. [20] studied the influence of airfoil shape, tip geometry, Re and chord length on the performance of Clark Y, GM15, GOE 417 and FX63-137 airfoils. The test was carried out only through the angles of attack in close proximity to the design angles of attack α_{Design} for the respective airfoils. The experimental evaluation depicted that GM15 indicated the highest L/D_{max} consequently being the best fit for 2-bladed turbines. Using experimental methods, Göçmen et al. [21] optimized the geometry of FX 63-137, S822, S834, SD2030, SG6043 and SH3055 airfoils and analyzed the aerodynamic performance of the airfoils using XFOIL tool. The research works proposed that by altering the geometry on the pressure side of the airfoil, the aerodynamic performance of the airfoil can be significantly improved to be used for wind turbine applications. Applicability of Eppler and XFOIL codes for aerodynamic analysis of airfoils have been evaluated by Somers et al. [22]. The observations promoted XFOIL and Eppler codes as one of the beneficial solution for evaluating the aerodynamic characteristics of airfoils. Pathike et al. [23] articulated the simple philosophy of BEM theory in designing blades for small scale horizontal axis wind turbines. To simulate the real world conditions Gur et al. [24] presented the need to incorporate the effects of drag C_d and tip losses F_i on the performance of rotor blades. Experimental analysis of wind turbine blades carried out by Saoke et al. [25] portrayed that Clark-Y airfoil being highly suitable for a wind speed range of 4-10 m/s, with a reasonable power coefficient C_p up to 0.26 at 10m/s. Collecutt et al. [26] investigated the effect of operating a wind turbine at non-optimized mean wind speeds. Rotor blades optimized for 6-8 m/s was tested for mean wind speeds of 10m/s. Results for 10m/s wind speed shows that the power predicted is 10% less than for the design conditions. The literature enumerates that the optimization of a wind turbine must be carried out for the mean annual wind speeds observed at the site of operation. Bayati et al. [27] detailed the procedure for testing scaled model in a typical wind tunnel facility. Treuren et al. [28] discussed the testing of the scaled down small-scale wind turbine system in a wind tunnel. Authors proposed the necessity of matching the Reynolds number for testing and evaluating the performance of scaled down models. Through detailed experimental assessment, Treuren et al. [29] furnished the guidelines for scaling the wind turbine blades for wind tunnel testing. As per the outcome, retaining the material, TSR, geometry, Reynolds number and the number of blades are very prerequisite for performing scaled down analysis. Experiments performed by Bottasso et al. [30] on scaled down wind turbine models showed that better power coefficients can be registered while operating a turbine between a TSR of 7-8. Chaudhary et al. [31] exploited the simplicity of Qblade numerical software, proving the utility of the software for designing and analysing the performance of a 400W wind turbine rotor blade. Jureczko et al. [32] initiated a comprehensive technique based on numerical method that proved to be a better technique for increasing the performance of any wind turbine. Minimization of rotational inertia through the utilization of wood material for the design of rotor blades have been presented by Singh et al. [33]

II. BLADE ELEMENT MOMENTUM THEORY

The blade element momentum theory (BEMT) has been dedicatedly developed for designing and analyzing the performance of horizontal axis wind turbine rotor blades, through the amalgamation of momentum and blade element theories, known as strip theory. Strip theory, treats the rotor blade as a combination of N number of elemental sections, wherein the global performance of the blade can be evaluated by integrating the performance of each elemental section. Among the various techniques, BEMT is quite widely used method for designing and analyzing a wind turbine blade. However, BEM theory has certain limitations as it underplays the effects of 3D flows, heavily loaded turbulent conditions, delayed stall, unsteady flows, yawed conditions etc.

Nevertheless, the practical approach of BEM theory in designing as well as analyzing the steady state performance of horizontal axis wind turbine rotor blade has proved the usefulness beyond any doubt. The theory of BEM is explained in the succeeding section.

A. Momentum Theory

BEM theory starts with the prediction of the net thrust forces induced on the wind turbine blade by the applying the conservation of linear momentum to the control volume as in figure 1.

$$T = \frac{1}{2}\rho A_2 (U_1^2 - U_4^2) \quad (1)$$

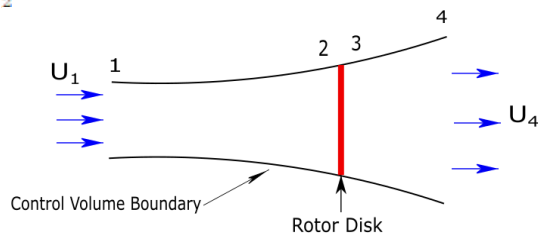

Fig.1. Control Volume Approach for a Wind Turbine Rotor Disk

The fractional decrease in the wind velocity as it approaches the rotor plane is termed as the Axial Induction Factor a and represented as

$$a = \frac{U_1 - U_2}{U_1} \quad (2)$$

Power from the wind in terms of axial induction factor is given by

$$P = \frac{1}{2}\rho A U^3\ 4a\,(1-a)^2 \quad (3)$$

Power and thrust coefficients of the wind turbine rotor blade are given by the below equations

$$C_P = 4a\,(1-a)^2 \quad (4)$$

$$C_T = = \frac{Thrust\ Force}{Dynamic\ Force} = \frac{T}{\frac{1}{2}\rho U^2 A} \quad (5)$$

To simulate the real working environment of a rotor blade, wake rotation ω behind an actual wind turbine has to be included in the BEM theory. The generation of angular momentum in the wake utilizes the energy from the rotor blade, therefore resulting in lower power output. The reduction in the angular momentum is defined by angular induction factor a'. The downstream wake occurring behind a real rotor blade is illustrated in figure 2.

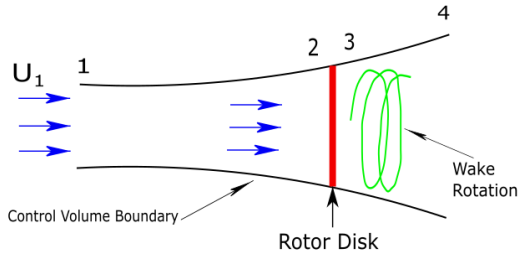

Fig.2. Representative Sketch for a Wind Turbine Model with Downstream Wake Rotation

Thrust in terms of a and a' acting on the annular element is given by

$$dT = 4a'(1+a')\frac{1}{2}\rho\Omega^2 r^2\, 2\pi r dr \quad (6)$$

Also, by considering the axial induction factor a and free stream velocity U, the equation for thrust can be

$$dT = 4a'(1-a)\frac{1}{2}\rho U^2 2\pi r dr \quad (7)$$

Equating the above two expressions for an annular element, we get

$$\lambda = \frac{\Omega R}{U} \quad (8)$$

Now, by applying the angular momentum conservation, the torque generated by an annular element of the blade is imparted by the expression

$$dQ = 4a'(1-a)\rho U \pi r^3 \Omega dr \quad (9)$$

The power generated by each element of the blade is

$$dP = \frac{1}{2}\rho A U^3 [\frac{8}{\lambda^2} a^1\ (1-a)\lambda_r^3 d\lambda_r] \quad (10)$$

The incremental power coefficient dC_P contributed by each annular element is

$$dC_p = \frac{dP}{\frac{1}{2}\rho A U^3} \quad (11)$$

Finally,

$$C_P = \frac{8}{\lambda^2}\int_0^{\lambda} a'(1-a)\lambda_r^3 d\lambda_r \quad (12)$$

The power produced by an actual rotor blade is always less compared to the blade without wake rotation. The same is outlined in figure 3.

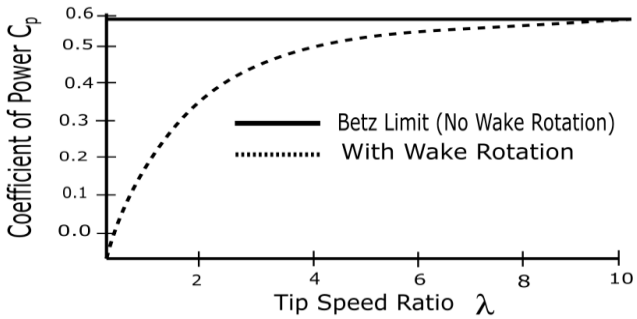

Fig.3. Illustration of Coefficient of Power C_p for Blade with and without Wake Rotation

B. Blade Element Theory

In the Blade element theory, the blade is divided into N elements as given in figure 4. Next, the forces on each element are calculated using the formulae derived by considering the lift and drag forces acting on the individual elements of the blade as given in figure 5.

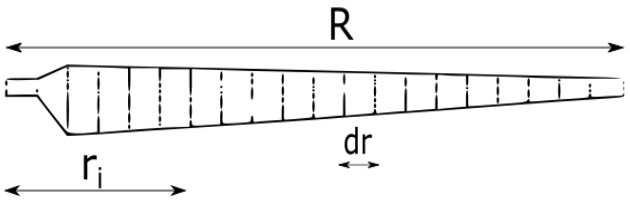

Fig.4. Schematic of a rotor blade

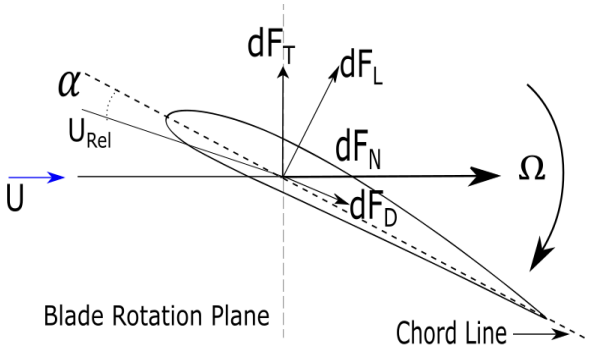

Fig.5. Primary Forces acting on the blade element

From the geometry, the following useful relations can be obtained.

$$\varphi = \theta_{p+} \alpha \quad (13)$$

$$tan\ \varphi = \frac{U(1-a)}{\Omega r(1+a')} = \frac{1-a}{(1+a')\lambda_r} \quad (14)$$

$$U_{rel} = \frac{U(1-a)}{sin\ \varphi} \quad (15)$$

$$dF_L = C_l \frac{1}{2} \rho U_{rel}^2 cdr \quad (16)$$

$$dF_D = C_d \frac{1}{2} \rho U_{rel}^2 cdr \quad (17)$$

$$dF_N = dF_L c cos\ \varphi + dF_D\ sin\ \varphi \quad (18)$$

$$dF_T = dF_L\ sin\ \varphi - cos\ \varphi \quad (19)$$

For a finite number of blades (B) considered, the normal force $d\ F_N$ and torque dQ occurring at a distance, r, from the axis of rotation are provided by combining the previous equations.

$$dF_N = B\frac{1}{2} \rho U_{rel}^2 (C_l\ cos\ \varphi + C_d\ sin\ \varphi) cdr \quad (20)$$

$$dQ = B\frac{1}{2} \rho U_{rel}^2 (C_l\ sin\ \varphi - C_d\ cos\ \varphi) crdr \quad (21)$$

Blade Element Momentum theory for determining the geometry and performance of a rotor blade is presented by the schematized flow chart in figure 6.

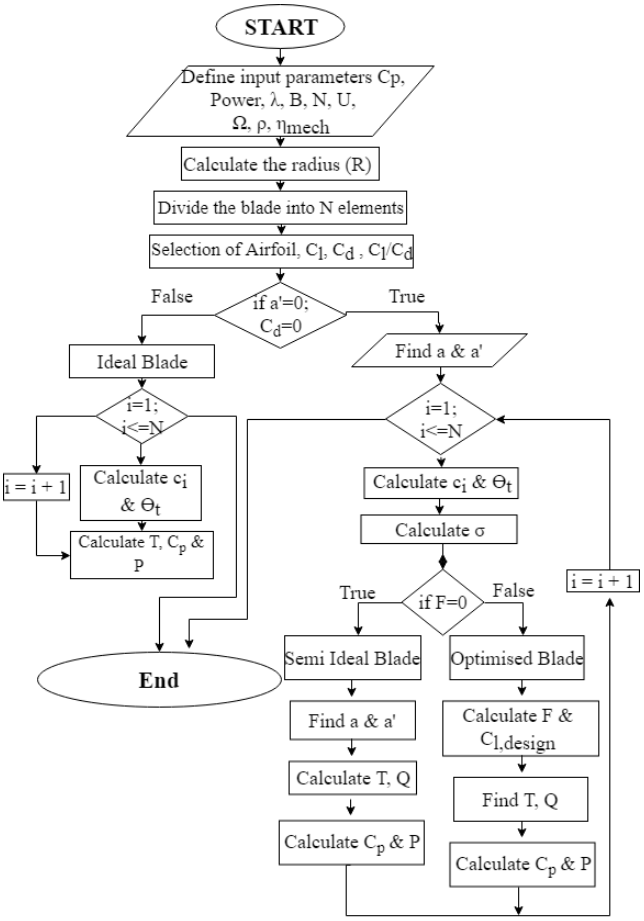

Fig.6. Flow chart of Blade Element Momentum Theory

As highlighted in the flow chart, designing a rotor blade is an iterative process. The sequence begins with the design of a preliminary idealized blade that will be optimized to suffice realistic flow conditions contemplating the effects of wake ω, drag C_d and tip losses F_i. Conclusively, the optimized blade will thereupon be remodified through linearization techniques.

C. Airfoils for Wind Turbine Rotor Blade

Choice of airfoils for wind turbine blade compulsorily requires satisfying two important criteria. The first criterion is to be as aerodynamically efficient as possible to generate maximum lift at the least value of drag that translates to high power output P_{max} . For this purpose, an airfoil exhibiting high aerodynamic efficiency (C_l/C_d) needs to be considered. The second criterion is to be structurally stable so that all the loads generated during the operation of the turbine will be transferred to the root section of the blade without undergoing any failure. As a general practice, the outer section (0.3-1R) of the blade is usually composed of thin airfoils with thickness less than 20% of the chord providing high lift. Similarly, the root section (0.05-0.3R) is made structurally strong by composing the blade with airfoils having thickness greater than 20%. The same has been highlighted in table 1 and the candidate airfoils for wind turbine application are listed in table 2.

Table I: Airfoil Selection Criteria for Rotor Blade Design

Section of the Blade	Blade Location in %	Type of Airfoils	Role of the Airfoil
Root Section	0-25%	Thick Airfoils	Load Bearing and Support Generate Required Torque
Primary Section	25%-75%	Moderately Thick Airfoils	Maximize Aerodynamic Efficiency Aid in useful Power Generation
Tip Section	75%-Tip	Thin Airfoils	

Table II: Airfoils for stall controlled Wind Turbines

Airfoil Name	Max Thickness	Location of max Thickness	Design Rey No	Max L/D	Alpha α_{Design}
A-18	7.3%	30%	$1*10^5$	65	4.5
BW-3	5%	7.4%	$1*10^5$	67.6	4.5
Clark-Y	11.7%	28%	$1*10^5$	53	6.75
GOE 417A	6%	20%	$1*10^5$	62	3.5
E387	9.1%	31.1%	$1*10^5$	60.7	7.5
S823	21.2%	24.3%	$1*10^5$	42.33	9.25
S822	16%	39.2%	$1*10^5$	42.69	8.5

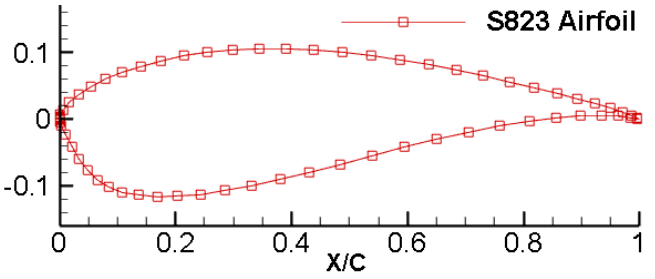

(a)

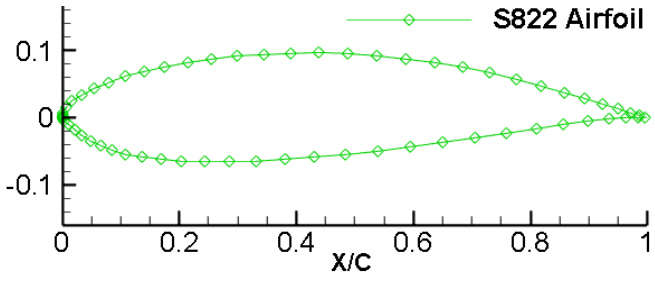

(b)

Fig.7. Representation of S823 and S822 NREL Airfoils

S823 and S822 airfoils endorsed by NREL have been incorporated to meet the geometrical conformity of the blade. S823 and S822 are highly specialized airfoils acceptable for wind turbines of capacities ranging from 2kW to 10kW [34]. The NREL S series airfoils are better known for Low Reynolds number performance in combination with insensitivity towards leading edge roughness [35]. The C_l and C_l/C_d graphs of S823 and S822 airfoils for a $Re=1*10^5$ have been tested via QBlade software and is displayed in figure 8. Table 3 tabulates the aerodynamic characteristics of both the airfoils attained through QBlade.

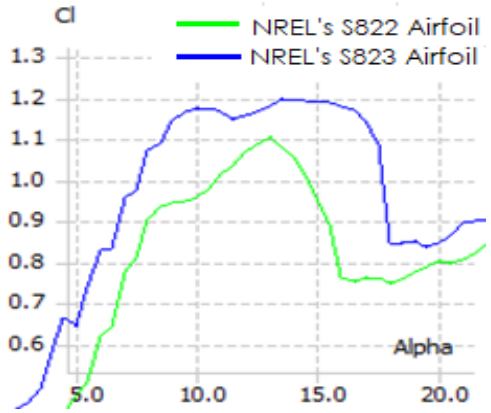

(a)

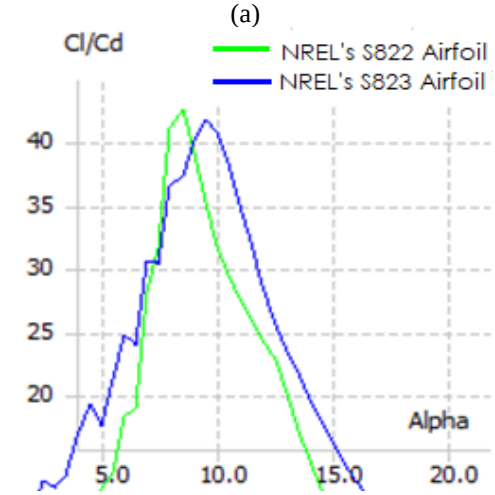

(b)

Fig.8. Coefficient of Lift C_l and C_l/C_d representation of S823 and S822 airfoils at $Re=1*10^5$

Table III: Aerodynamic Characteristics of S823 & S822 Airfoils

Aerodynamic Parameters	QBlade Results at $Re=1*10^5$	
	S823	S822
$C_{l\,max}$	1.157	0.926
α_{max}	15^0	13^0
C_l/C_d	42.23 at 9.25^0	42.69 at 8.5^0
$C_{d\,min}$	0.02733 at 9.00^0	0.02167 at 8.25^0

D. Wind Turbine Specifications

The wind turbine system considered encompasses the specifications highlighted in the table 4:

Table IV: Wind Turbine Specifications

Type	Horizontal axis-Upwind	**Hub radius (R_b)**	0.1 m
Rated Power (P)	2kW	**Number of blades (B)**	3
Rated wind speed (V)	10m/s	**Design tip speed ratio (λ)**	7
Rotor Radius (R)	1.6 m	**Airfoils Used**	S823 (Root: 0-30%)
Rotor Diameter (D)	3.4 m		S822 (Primary: 30%-Tip)

III. ANALYTICAL DESIGN OF ROTOR BLADE

A. Step 1 : Design of Rotor Blade without Wake Rotation-Idealized Rotor Blade

Initially, idealized rotor blade geometry for the stated power and flow conditions has to be determined by excluding the effect of wake rotation, drag and tip losses i.e., $\omega = C_d = F_i = 0$. Besides, the axial induction factor is assumed to be a constant (a=1/3) throughout the geometry of the blade. From BEM theory, following expressions is applied to determine the geometrical properties of the idealized blade.

Angle of Relative Wind

$$\varphi_i = tan^{-1}\left(\frac{2}{3\lambda_{r,i}}\right) \quad (21)$$

Sectional Chord Distribution

$$c_i = \frac{8\pi r_i}{3B\lambda_{r,i}C_{l,design,i}}(Sin\varphi_i) \quad (22)$$

Sectional Twist Distribution

$$\theta_{T,i} = \theta_{p,i} - \theta_{p,0} \quad (23)$$

$$\varphi_i = \theta_{p,i} + \alpha_{design,i} \quad (24)$$

Table V: Geometrical Properties of the Idealized Rotor blade

Blade Station r_i (m)	**Relative Wind Angle** φ_i (Deg)	**Sectional Chord** c_i (m)	**Sectional Pitch Angle** $\theta_{p,i}$ (Deg)	**Sectional Twist Angle** θ_{Ti} (Deg)
0.08	62.32	0.492	53.07	56.12
0.16	43.62	0.383	34.37	37.43
0.24	32.43	0.298	23.18	26.23
0.32	25.48	0.239	16.23	19.28
0.40	20.87	0.198	11.62	14.67
0.48	17.62	0.210	9.12	12.18
0.56	15.23	0.182	6.73	9.79
0.64	13.40	0.161	4.90	7.96
0.72	11.96	0.144	3.46	6.51
0.81	10.79	0.130	2.29	5.35
0.89	9.83	0.119	1.33	4.39
0.97	9.02	0.109	0.52	3.58
1.05	8.34	0.101	-0.16	2.90
1.13	7.75	0.094	-0.75	2.31
1.21	7.24	0.088	-1.26	1.80
1.29	6.79	0.082	-1.71	1.35
1.37	6.40	0.077	-2.10	0.95
1.45	6.04	0.073	-2.46	0.60
1.53	5.73	0.069	-2.77	0.28
1.61	5.44	0.066	-3.06	0.00

Parametric influence of flow velocity U, number of blades B, the coefficient of lift C_l for the airfoil chosen, an idealized blade presenting a taper and twisted geometry is obtained. The angle of relative wind φ_i, sectional chord distribution c_i, sectional pitch angle θ_{pi}, and sectional twist θ_{Ti} for the idealized blade are arrived and tabulated in table 5.

Chord is a predominant parameter in the geometrical design of a rotor blade. The geometry of the idealized rotor blade obtained through BEMT is presented in figure 9 and the variation in the sectional chord distribution c_i from root to tip is shown in figure 10a. Figure 10a evinces that the idealized blade displays a maximum chord c_i=0.492m at root r_i=0.0805m from the hub which then tapers off gradually to the least value of c_i=0.066m at the tip where r_i=*1R*. The geometry rendered to the idealized rotor blade is in accordance with the structural and aerodynamic prerequisite. The root portion of the blade is sufficiently large to withstand the loads effectuated on the blade during the operation. Likewise, as the radius graduates from the root, the chord length tapers, exhibiting an efficient design capable of generating high aerodynamic forces in conjunction with least drag. This would have been untrue, if the chord c_i had remained constant without the provision of any taper. It can be seen from the figures 9 and 10a that the idealized blade displays an uneven distribution across 0.25R to 0.35R rendering a slightly jagged appearance. The non-interpolation of the transition region through the semi span 0.25R to 0.35R is solely responsible in contributing to an uneven chord distribution across the said region. Far off the transition side, the variation in the chord distribution is fairly soother and linear.

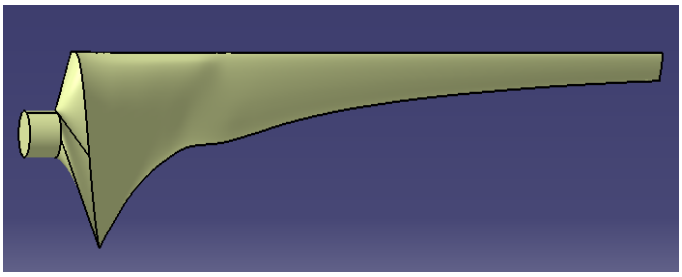

Fig.9. Illustration of Idealized Rotor Blade

Blade twist θ_{Ti} is another significant geometrical parameter deciding the structural, hence the performance of the blade. Similar to the chord distribution c_i, the maximum twist θ_{Ti} occurs at the root of the blade. At r_i=*0.05R* the blade displays a highest twist of 53^0 which then drastically untwists itself to -3^0 at r_i=*1R*. During operation, the relative velocity U_{rel} experienced by the rotor blade varies distinctly from the root to the tip. The outer portion (0.3R to 1R) experiences significantly higher relative velocity in comparison to the root section (0.1R to 0.3R) of the blade. The varying relative velocity induces an asymmetric lift distribution through the span of the blade resulting in a lopsided aerodynamic loading on the blade. To avoid this undesirable consequence, BEM theory automatically predicts large values of twist at the regions closer to the root. Twisting the blade to higher angles proportionately increases the lift produced. Hence, provision of a sectional twist aids is maintaining a fairly moderate lift throughout the blade and at the same time suffices the structural requirement of the blade. The geometrical sectional twist θ_{Ti} of the idealized blade at various radial locations is prominently shown in figure 10b.

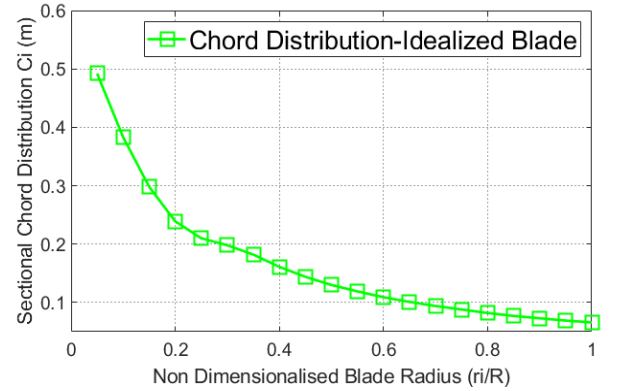

(a)

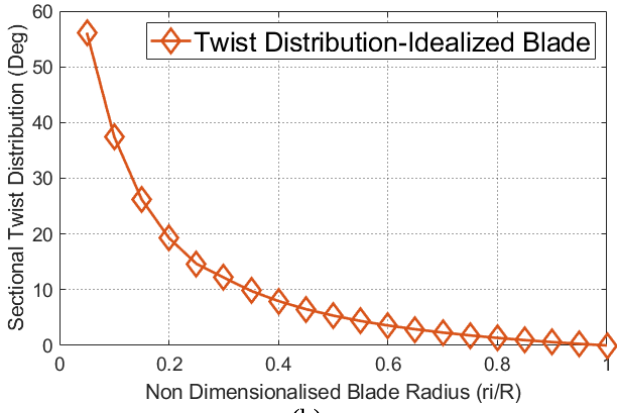

(b)

Fig.10. Variation of Chord c_i and Twist Distribution θ_{Ti} of the Idealized Blade

B. Step 2 : Design of Rotor Blade with Wake Rotation ω-Optimized Rotor Blade

Mathematical formulations of BEM theory for an optimum blade are slightly altered to contain the influences of wake ω, drag C_d and tip losses F_i. The resulting geometry for the optimized blade is obtained from equations 25 & 26.

Angle of Relative Wind

$$\varphi_i = \left(\frac{2}{3}\right) tan^{-1} \left(\frac{1}{\lambda_{r,i}}\right) \quad (25)$$

Sectional Chord Distribution

$$c_i = \frac{8\pi r_i}{BC_{l,design,i}}(1-\cos\varphi_i) \quad (26)$$

The geometrical sectional properties for the optimized are given in the table 6.

The optimized blade obtained from BEM analysis is illustrated as a 3D model showcased in figure 11. The figure clearly illustrates a smoother geometrical distribution from root to the tip that is not observable on the idealized blade. The radial chord wise distribution c_i for the optimized blade has been supported by figure 12a. The chord for the optimized blade is seen to start at 0.18m from the root where r_i=*0.05R*. Next, the chord is found to increase to c_i=0.22m at the second element of the blade at *0.1R*, which then declines immediately past *0.15R*. Down span, the chord tapers off gradually to a minimum chord at r_i=*1R*. As expected, the least value of chord occurred at the tip with the value of c_i=0.065m. Important aspect that is little different from the idealized blade is a more even distribution of the chord across the transition region from *0.25R* to *0.35R*. Here the transition section has been gradually smoothened by interpolating the section through *0.25R* to *0.35R* rendering a linear distribution of the chord c_i and is vividly noticeable from the figure 12a.

Table VI: Geometrical Properties of the optimized rotor blade

Blade Station r_i (m)	**Relative Wind Angle** φ_i(Deg)	**Sectional Chord** c_i (m)	**Sectional Pitch Angle** $\theta_{p,i}$ (Deg)	**Sectional Twist Angle** θ_{Ti} (Deg)
0.0805	47.15	0.186	37.90	40.97
0.161	36.68	0.231	27.43	30.51
0.242	29.08	0.220	19.83	22.91
0.322	23.70	0.197	14.45	17.53
0.403	19.84	0.173	10.59	13.67
0.483	16.98	0.191	8.48	11.56
0.564	14.81	0.169	6.31	9.39
0.644	13.11	0.152	4.61	7.69
0.725	11.75	0.137	3.25	6.33
0.805	10.64	0.125	2.14	5.21
0.886	9.71	0.115	1.21	4.29
0.966	8.93	0.106	0.43	3.51
1.047	8.27	0.098	-0.23	2.85
1.127	7.69	0.092	-0.81	2.27
1.208	7.19	0.086	-1.31	1.77
1.288	6.75	0.081	-1.75	1.33
1.369	6.36	0.076	-2.14	0.94
1.449	6.02	0.072	-2.48	0.59
1.530	5.70	0.069	-2.80	0.28
1.610	5.42	0.065	-3.08	0.00

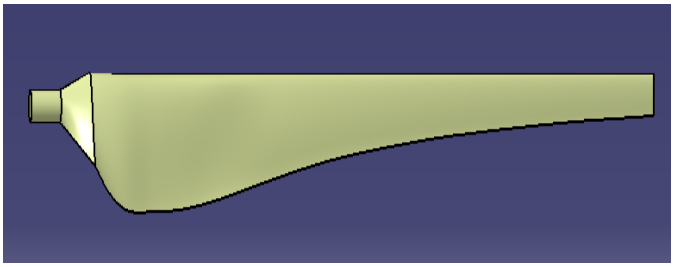

Fig.11. CATIA Model of the Optimized blade

Alongside the chord, the optimum blade also registers notable changes in twist distribution θ_{Ti}, detailed in figure 12b. Contrastingly it is apparent that the twist of the optimum blade no longer follows the distribution described by the idealized blade. The appreciable deviation in the twist occurs at the root section of the blade between *0.05R* to *0.35R*. The first element of the blade exhibits a maximum twist angle of 40.97 degrees followed by 30.51, 22.91, 17.53, 13.67 and 11.56 degrees until the sixth element. Incidentally, variation in the twist is very drastic up to the sixth element of the blade (*0.3R*), beyond which the twist gradually declines and ultimately ceases to 0 degrees at r_i=*1R*.

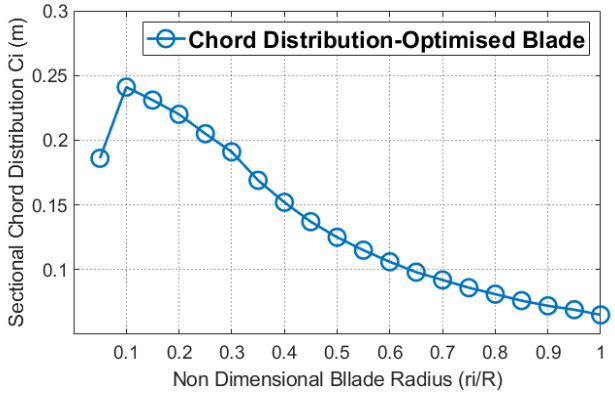

(a)

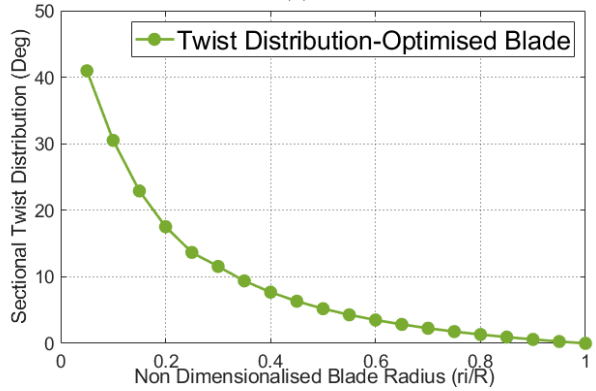

(b)

Fig.12. Variation of Chord c_i and Twist Distribution θ_{Ti} of the Optimized Blade

C. Step 3 : Linearization of the Rotor Blade

Linearizing the blade profile is the last step in the design of a more realizable blade for a horizontal axis wind turbine blade. Linearizing the blade profile leads to a simpler geometry that eases the manufacturing complexity and eventually reduces the cost of production of the blades [36]. Linearization has become a standard strategy widely adopted in the wind turbine industry. Different authors have proposed standalone theories to linearize the blade. Nonetheless, in the present work an uncomplicated MATLAB code has been used to linearize the chord and twist angles of the optimized blade [39].

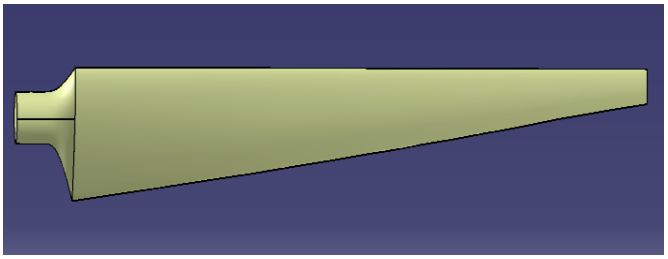

Fig.13. Rotor blade linearized for chord and twist

An easy yet effective two point scheme has been employed to accomplish the linearization technique. Linearization of the blade profile is elucidated by a single degree polynomial expression as demonstrated by the equation $f(x) = p_1 x + p_2$, where, p_1 and p_2 are constants obtained from the graphical values. The MATLAB code projected a simple linear curve of best fit by optimizing the slopes of the chord c_i and twist angles θ_{Ti} at multiple radial locations of the blade from radius r_i=*0.05R* to *1R*. The linearized slope for blade chord c_i and twist angles θ_{Ti} were obtained by joining the root chord to the tip chord and root twist angles to the tip twist angles respectively. Numerous linearized curves can be obtained by selecting various points along the span where the linearization treatment is necessary. The blade profile can be linearized along the entire span or between any two local points along the span. In this work, the blade profile has been linearized through the entirety of the blade span from $r_i / R = 0$ to $r_i / R = 1$. The CATIA model of the linearized blade achieved is shown in figure 13. The linearized sectional chord c_i and twist distribution θ_{Ti} obtained through the two point scheme in MATLAB are given in figure 14.

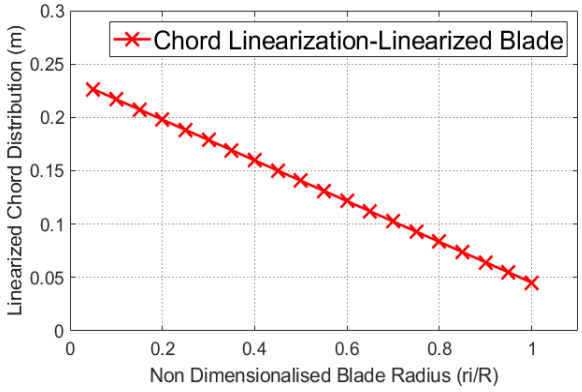

(a)

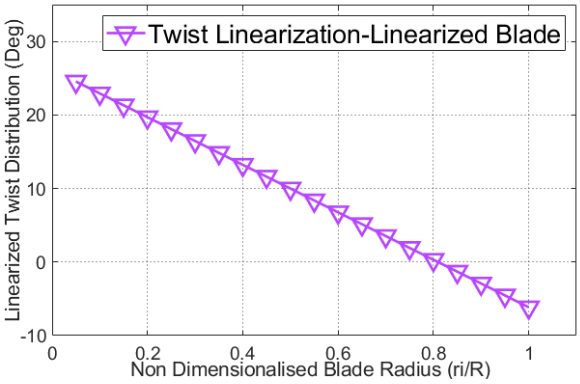

(b)

Fig.14. Linearized Sectional Chord c_i and Twist θ_{Ti} with Non Dimensionalised Blade Radius r_i/R

IV. RESULTS AND DISCUSSIONS

Heuristic nature of the BEMT in achieving an aerodynamically as well as structurally optimum rotor blade for small sale horizontal axis wind turbine has been employed. Initially, with the aid of BEM theory, a preliminary idealized blade has been designed ignoring the effects of wake rotation, drag and tip losses. Next, to include the detrimental effects of wake and drag the BEM theory has been slightly remodified to accomplish an optimum blade design. In the final step, practically achievable blade design has been obtained using a linearization technique. Figure 15a shows the comparison between the chord variations c_i for idealized, optimized and linearized blades. It is visually evident from the figure that the linearized blade depicts an unpretentious geometry especially across the root section as juxtaposed against the idealized and optimized blades.

Idealized blade exhibits a maximum chord c_i = 0.49m at $r=0.05R$ as compared to just 0.18m of the optimized blade and 0.22656m of the linearized blade translating to 62.09% and 53.92% decrease in the blade geometry of the optimized and linearized blades independently. The trend in the geometry reduction continues with progressing r_i from 0.05R to 0.4R. But, beyond 0.4R the percentage curtailment in the geometry becomes sluggish and all three blades exhibit an almost similar trend as noticed in figure 15a.

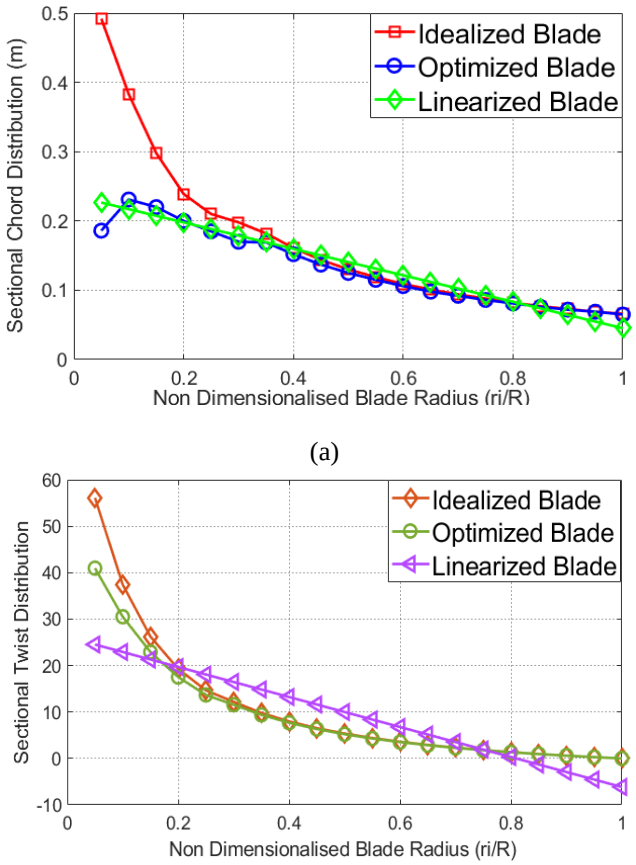

Fig.15. Comparison of Sectional Chord Distribution c_i and twist distribution θ_{Ti} for all three blades

Identically, the twist distribution of the idealized blade also represents a similar case of chord variation. From figure 15b it can be obvious that the idealized blade possesses large twist angles across the root section from *0.05R* to *0.3R*. Post *0.3R* the slope of the twist angle slowly falls with increasing radius r_i and linearly approaches almost a constant value farther beyond *0.6R*. On the other hand, the variation in the local twist angles θ_{Ti} of the optimized blade depicts a similar trend as represented by the idealized blade. The local twist angle of the optimized blade at *0.05R* is 40.97^0 as in comparison with θ_{Ti}= 56.12^0 of the idealized blade which is 26.99% less than the idealized blade. The twist angle of the optimized blade continues to decrease with the local radius r_i. Variation in the twist angle of the optimized blade is noteworthy only up to *0.2R* after which the variation in the twist angle exactly harmonizes with the idealized blade twist variation. However, the linearized blade establishes a twist distribution that is distinctively different from the idealized as well as the optimized blades.

The variation in the chord and twist distribution is in regards to the BEM philosophy. As BEM theory neglects all losses under ideal operating environment, the idealized blade tries to simulate maximum power output P_{max} for any given inflow conditions. In this regard, the BEM theory predicts large values of chord and twist distribution through the entirety of the blade span. Manufacturing a blade with large values of chord and twist supposedly invites a situation requiring special manufacturing techniques that further leads to higher production, operational and maintenance costs of the blade. But, linearizing the blade drastically eases the blade geometry which manifests restrained values of chord c_i and θ_{Ti} twist distribution right through the span of the blade. The lighter geometry of the linearized blade is comparatively easier to fabricate without escalating the manufacturing and maintenance costs of the blades.

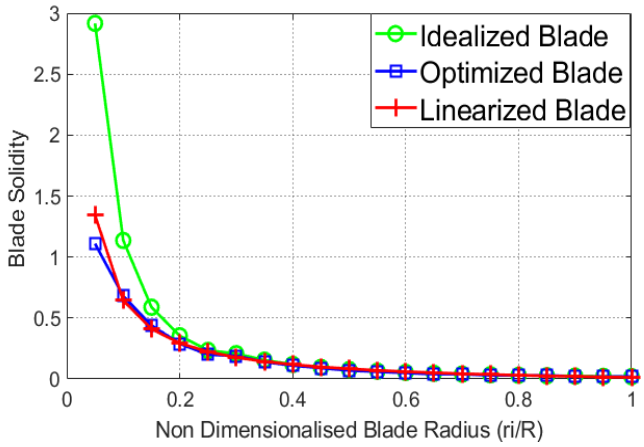

Fig.16. Comparison of Solidity of Idealized, Optimized and Linearized blades

The geometrical configuration of the rotor blade has a crucial influence on the solidity of the blade that affects the performance of the wind turbine. Solidity is the ratio of the planform area of the blades to the swept area and mathematically defined as $\sigma = Bc/2\pi r$. For electrical wind turbines, the relation impresses upon the demand for blades with low solidity that translates into higher rotational velocities and better power output. The variation of solidity for all three blades is portrayed in figure 16. Since, the idealized blade predicts large chord distribution c_i, solidity is incomparably the highest as discerned from figure 16. Undoubtedly, the solidity will be maximal at the root section from 0.05R to 0.3R where the concentration of the chord geometry is large. With the chord declining, the local solidity σ' of the all the blades show a drastic reduction up to 0.3R. Afterwards, the solidity manifested by all three blades nearly coincides as indicated in figure. The average solidity for the idealized blade measured σ=0.3122 as compared to the optimized blade with σ=0.2127. Likewise, the linearized blade with comprehensible geometry manifested lowest solidity of σ=0.1953. Comparably the idealized blade demonstrated a solidity that is 31.8% and 37.44% higher than the optimized and linearized blades separately. The reduction in the solidity may prove beneficial for the linearized blade in terms of better TSR, power coefficients C_p and many more.

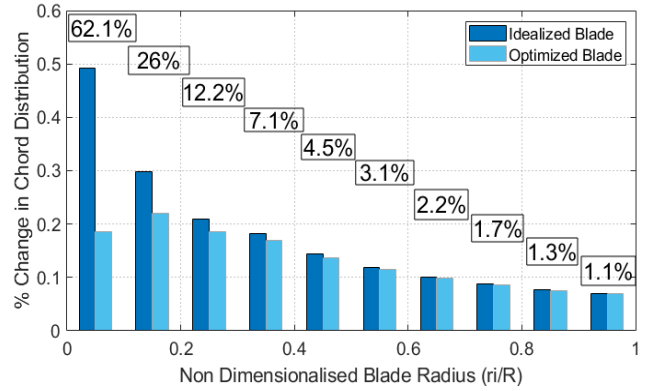

(a)

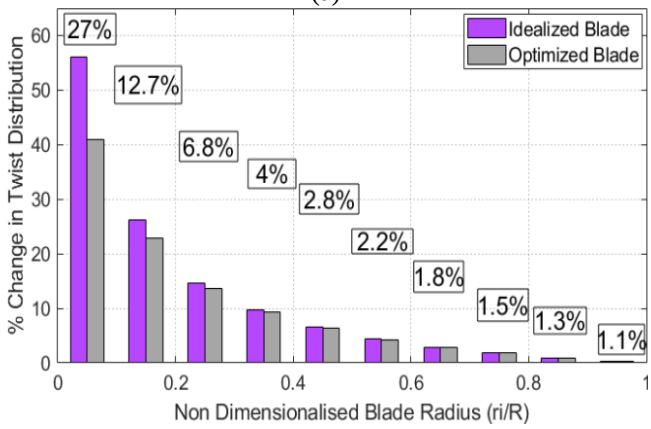

(b)

Fig.17. Percentage Variation in chord c_i and twist distribution θ_{Ti} for Idealized and Optimized blades

Lastly, figures 17 and 18 shows percentage difference in chord c_i and twist distribution θ_{Ti} between the three blades. Dominant area of focus is towards the root section of the blade that depicts the maximum change in the chord and twist distribution. The prominent change described by the idealized blade is in relation with the optimum power conditions that require the geometry to be large. Regardless, due to the off-design factors, the performance predicted by the idealized blade will not necessarily be higher at all the operating conditions [38]. Hence, large chord and twist distributions are not dictum factors for better performance of the blade. Linearization aids in a modest blade geometry with undemanding fabrication processes and lower production costs, yet providing power comparable with the optimized blade [39].

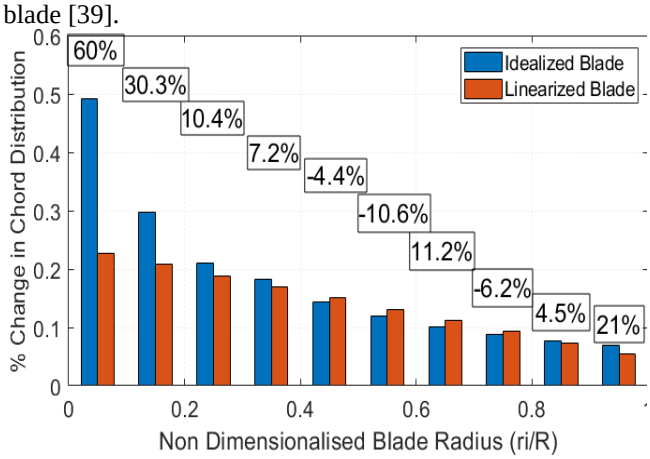

(a)

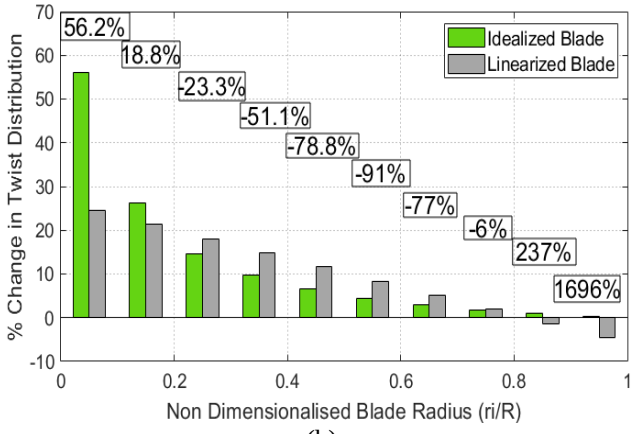

(b)

Fig.18. Percentage variation of chord c_i and twist distribution θ_{Ti} for Idealized and Linearized blades

V. CONCLUSIONS

In the present work, an elaborate analytical iterative sequences involved in the geometrical design of a rotor blade for a small 2kW horizontal axis wind turbine using BEM theory has been undertaken. Through BEM articulation, a preliminary idealized blade capable of generating maximum power has been attained. The geometrical complexity exhibited by the idealized blade imposes severe fabrication challenges that cannot be achieved using any off-the-shelf fabrication technique. Nevertheless, the idealized blade facilitates the essential bridging between the hypothetical and practical blade. Lastly, linearization forms the final step in the design process culminating in a blade that is more conceivable within the bounds of cost effective manufacturing limitations.

REFERENCES

1. Björn Pieprzyk, Norbert Kortlüke, Paula Rojas Hilje "The impact of fossil fuels Greenhouse gas emissions, environmental consequences and socio-economic effects" Energy Research Architecture, November 2009.
2. Adam Sieminski, "World Energy Outlook", International Energy Forum, September 9, 2018
3. BP Statistical Review of World Energy, 67th Edition, 2018
4. American Coalition for Clean Coal Electricity, "The Social Costs of Carbon? No, the Social Benefits of Carbon" January 2014
5. Corinne Le Quéré, Robbie M. Andrew, Josep G. Canadell, "Global Carbon Budget-2016", Earth Syst. Sci. Data, 8, 605–649, 2016, doi:10.5194/essd-8-605-2016
6. Virginie Marchal, Rob Dellink, Detlef van Vuuren, Christa Clapp, Jean Château, Eliza Lanzi, Bertrand Magné, Jasper van Vliet, "OECD Environmental Outlook to 2050" November 2011
7. International Energy Agency, "Global Energy & CO2 Status Report", 2017
8. Dr. Abdullah Karatas, "Environmental Impacts of Globalization and a Solution Proposal", American International Journal of Contemporary Research, Vol. 6, No. 2; April 2016
9. Phebe Asantewaa Owusu, Samuel Asumadu-Sarkodie, "A review of renewable energy sources, sustainability issues and climate change mitigation" Cogent Engineering (2016), 3: 1167990
10. 2017 Wind Technologies Market Report, U.S Department of Energy
11. J. Manwell, A. L. Rogers and J. G. McGowan, Wind Energy Explained Theory, Design and Application, 2nd ed., Chichester, West Sussex: John Wiley & Sons, Ltd., 2009.
12. Global Wind Energy Council, "Global Wind Statistics" 2017
13. Sandip. A. Kale, Ravindra N. Varma, "Aerodynamic Design of a Horizontal Axis Micro Wind Turbine Blade Using NACA 4412 Profile", International Journal of Renewable Energy Research, Vol. 4, No. 1, 2014

14. Rohit Kumar Gupta, Vilas Warudkar, Rajesh Purohit, Saurabh Singh Rajpurohit, “Modeling and Aerodynamic Analysis of Small Scale, Mixed Airfoil Horizontal Axis Wind Turbine Blade” 6th International Conference of Materials Processing and Characterization (ICMPC 2016), Materials Today: Proceedings 4 (2017) 5370–5384
15. Prasad, Navin, S. Janakiram, T. Prabu, S. Sivasubramaniam. "Design and development of horizontal small wind turbine blade for low wind speeds" International Journal of Engineering Science & Advanced Technology, Volume-4, Issue-1, 075-084, ISSN: 2250-3676
16. Burdett, Tim, Jason Gregg, and Kenneth Van Treuren, "An examination of the effect of Reynolds number on airfoil performance", ASME 2011 5th International Conference on Energy Sustainability, pp. 2203-2213. American Society of Mechanical Engineers, 2011
17. Chaudhary, Umesh, and Sisir Kumar Nayak. "Micro and small-scale HAWT blades airfoils study through CFD for low wind applications" In 2015 Annual IEEE India Conference (INDICON), pp. 1-6. IEEE, 2015.
18. Vipin Kumar Satankar, Dr. Vilas Warudkar, "Modeling and aerodynamic analysis of small scale, mixed airfoil HAWT blade: A Review." International Research Journal of Engineering and Technology (IRJET), 2016.
19. Giguere, P., and Michael S. Selig. "New airfoils for small horizontal axis wind turbines." Journal of solar energy engineering 120, no. 2 (1998): 108-114.
20. Wisniewski, Charles F., Aaron R. Byerley, William H. Heiser, Kenneth W. Van Treuren, and William Liller III. The Influence of Airfold Shape, Tip Geometry, Reynolds Number and Chord Strength on Small Propeller Performance and Noise. USAF Academy Colorado Springs United States, 2015.
21. Göçmen, Tuhfe, and Barış Özerdem. "Airfoil optimization for noise emission problem and aerodynamic performance criterion on small scale wind turbines." Energy 46, no. 1 (2012): 62-71.
22. Somers, D. M., and M. D. Maughmer. Theoretical Aerodynamic Analyses of Six Airfoils for Use on Small Wind Turbines: July 11, 2002--October 31, 2002. No. NREL/SR-500-33295, National Renewable Energy Lab.(NREL), Golden, CO (United States), 2003.
23. Pathike, Paramet, Thanad Katpradit, Pradit Terdtoon, Phrut Sakulchangsatjatai. "A new design of blade for small horizontal-axis wind turbine with low wind speed operation." Energy Research Journal Volume 4, Issue 1, Pages 1-7, DOI: 10.3844/erjsp.2013.1.7
24. Gur, Ohad, Aviv Rosen. "Optimal design of horizontal axis wind turbine blades" ASME 2008 9th Biennial Conference on Engineering Systems Design and Analysis, pp. 99-109, American Society of Mechanical Engineers, 2008.
25. [Saoke, C. O., and Y. Nishizawa. "Design And Fabrication And Testing of a Low Speed Wind Turbine Generator Using Tapered Type Rotor Blade Made From Fibre Reinforced Plastic." International Journal of Renewable and Sustainable Energy, 2014; 3(1): 20-25, doi: 10.11648/j.ijrse.20140301.1
26. Collecutt, G. R., and R. G. J. Flay. "The economic optimisation of horizontal axis wind turbine design." Journal of wind engineering and industrial aerodynamics 61, no. 1 (1996): 87-97.
27. Bayati, Ilmas, Marco Belloli, Luca Bernini, Alberto Zasso. "Aerodynamic design methodology for wind tunnel tests of wind turbine rotors." Journal of Wind Engineering and Industrial Aerodynamics 167 (2017): 217-227.
28. Van Treuren, Kenneth W., Jason R. Gregg. "Testing of Rotating Horizontal Axis Wind Turbine Blade Designs in a Laboratory Wind Tunnel" In ASME Turbo Expo 2010: Power for Land, Sea, and Air, pp. 901-909. American Society of Mechanical Engineers, 2010
29. Van Treuren, K. W., and Hays, A. W., 2017, “Understanding, Designing, and Initial Testing of Small-Scale Horizontal Axis Wind Turbines for the Urban Environment,” Proceedings of the 1st Global Power and Propulsion Forum, Jan 16-18, 2017
30. Bottasso, Carlo L., Filippo Campagnolo, Vlaho Petrović. "Wind tunnel testing of scaled wind turbine models: Beyond aerodynamics." Journal of wind engineering and industrial aerodynamics 127 (2014):11-28.
31. Chaudhary, Manoj Kumar, Anindita Roy. "Design & optimization of a small wind turbine blade for operation at low wind speed." World Journal of Engineering 12(1) (2015) 83-94, ISSN: 1708-5284
32. Jureczko, M. E. Z. Y. K., M. Pawlak, and A. Mężyk. "Optimisation of wind turbine blades" Journal of materials processing technology 167, no. 2-3 (2005): 463-471.
33. Singh, Ronit K., and M. Rafiuddin Ahmed. "Blade design and performance testing of a small wind turbine rotor for low wind speed applications." Renewable Energy 50:812-819, February 2013, DOI: 10.1016/j.renene.2012.08.021
34. J. L. Tangier, D. M. Somers, “NREL Airfoil Families for HAWTs”, January 1995 • NREL/TP-442-7109
35. Christopher A. Lyon, Andy P. Broeren, Philippe Giguere, Ashok Gopalarathnam, Michael S. Selig, “Summary of Low-Speed Airfoil Data” Volume 3, SoarTech Publications, Virginia Beach, Virginia
36. Shubham Deshmukh, Manabendra M. De, “Investigation of Blade Geometry Linearization on Performance of Small Wind Turbine”, 61st Congress of the Indian Society of Theoretical and Applied Mechanics, 11-14 December 2016, Vellore, Chennai
37. Xiongwei Liu, Lin Wang, Xinzi Tang, “Optimized linearization of chord and twist angle profiles for fixed-pitch fixed-speed wind turbine blades”, Renewable Energy 57 (2013) 111-119
38. Xiongwei Liu, Lin Wang, Xinzi Tang, Optimized linearization of chord and twist angle profiles for fixed-pitch fixed-speed wind turbine blades, Renewable Energy 57 (2013) 111e119
39. M.T. Velázquez, M.V.Carmen, J.A.Francis, L.A.Pacheco and G.T.Eslava, Design and Experimentation of a 1 MW Horizontal Axis Wind Turbine, Journal of Power and Energy Engineering, (2013).

AUTHORS PROFILE

Supreeth R, working as Assistant Professor at Department of Aerospace Engineering, R V College of Engineering, Bangalore, India. Having an academic experience of nearly 7 years, the author is focused towards the design and development of Small Scale Horizontal Axis Wind Turbines, besides, working on research areas related to flow separation and its control.

Dr A Arokkiaswamy is currently heading the Department of Aeronautical Engineering at Dayananda Sagar College of Engineering, Bengaluru. The author has a rich Industrial and Research experience of around 35 Years. Primary area of research includes Low as well as High Speed Aerodynamics in conjunction with Propulsion and authored numerous scientific articles in the said field.

Nagarjun J Raikar, final year student in the Department of Aerospace Engineering, R V College of Engineering, Bengaluru. His field on interest includes wind energy, hybridization of wind energy and solar energy.

Prajwal H P, final year student in the Department of Aerospace Engineering, R V College of Engineering, Bengaluru. Prajwal field of interests include Aerodynamics, Understanding Flow Separation, Boundary Layer Phenomenon and its associated problems.

Sudhanva M, final year student in the Department of Aerospace Engineering, R V College of Engineering, Bengaluru. Sudhanva is well versed with design and modeling coupled with numerical analysis of flow over bodies. His expertise also includes analysis of dynamically rotating structures such as wind turbines.